SEISMICITY AND TECTONICS OF THE NINETYEAST RIDGE AREA: EVIDENCE FOR INTERNAL DEFORMATION OF THE INDIAN PLATE

Seth Stein and Emile A. Okal

Seismological Laboratory, California Institute of Technology, Pasadena, California 91125

Abstract. The Ninetyeast Ridge, far from being 'aseismic', has historically been a region of substantial seismicity. Since 1913, 4 magnitude 7 or greater earthquakes (including one with M_S = 7.7) and 10 magnitude 6 events have occurred in this general area. We have determined the mechanisms of several of these earthquakes, which suggest that the Ninetyeast Ridge area is presently a complex zone of deformation within the Indian plate. The northern portion (3°N-10°S) of the ridge is the active seismic zone, where both vertical and strike slip motion occur, while further south the ridge is far less seismic. This transition roughly coincides with a change in the ridge's morphology from irregular en échelon blocks to a smooth flat-topped high. The strike slip motion is left lateral, which is consistent with the Indian (west) side encountering resistance due to the collision with Asia while the Australian (east) side is subducting smoothly at the Sumatra trench. South of about 9°S the style of deformation differs on the two sides of the ridge. To the east, normal faulting occurs, which may be related to the formation of grabenlike structures. To the west the topography can be interpreted as the result of NW-SE compression which takes place largely aseismically but is observed for one large earthquake. This signficant intraplate deformation may explain the difficulties that occur in attempts to close the India-Africa-Antarctica triple junction using a rigid Indian plate.

Introduction

The Ninetyeast Ridge in the eastern Indian Ocean is a long linear feature extending from about 9°N to about 31°S. Its northern portion separates the thick sediments of the main Bengal fan from its eastern lobe, the Nicobar fan [Curray and Moore, 1974]. In this region (extending to about 7°S) the ridge is broken up into a complex series of en échelon blocks, while further south the ridge is straight and flat topped [Sclater and Fisher, 1974]. The east side of the ridge is bordered by a fracture zone and a complex of ridges and grabenlike troughs approximately parallel to the ridge [Bowin, 1973]. West of the ridge (and south of 7°S) a complex terrain composed of northeast trending ridges and deeps appears, along with a broad bathymetric high (15°S, 87°S) named Osborne Knoll by Sclater and Fisher [1974].

Ever since the Ninetyeast Ridge's true extent was recognized during the International Indian Ocean Expedition (1960-1965) its origin and nature have been subjects of intense discussion. It has been interpreted alternately as a horst [Francis and Raitt, 1967], as the result of overthrusting [Le Pichon and Heirtzler, 1968], as a hot spot trace [Morgan, 1972], as being due to localized emplacement of gabbro [Bowin, 1973], and as a volcanic pile generated at the intersection of a ridge crest and a transform fault [Sclater and Fisher, 1974]. Sclater and Fisher showed that magnetic anomalies to the west of the ridge age to the north, while to the east they age to the south. They also found that the ridge was attached to the Indian plate and bounded by a transform fault to the east during the Tertiary. The reason for the ridge's elevation above the ocean floor is also in dispute. Sclater and Fisher [1974] and Detrick et al. [1977] show that the ridge is subsiding at the normal rate for oceanic crust and is thus not an actively maintained feature. Paleontological studies of Deep Sea Drilling Project cores [Luyendyk and Davies, 1974] show that the ridge was formed at or above sea level, and the paleomagnetic data [Cockerham et al., 1975; Peirce, 1978] indicate that the ridge was formed at a high southern latitude. Models involving one [Peirce, 1978] or two [Luyendyk and Rennick, 1977] hot spots have been proposed to fit these data and explain the origin of the ridge. It is usually assumed that motion along the Ninetyeast Ridge ended 32 m.y. ago (anomaly 11), and that since then the Indian and Australian plates have been acting as a single plate.

Whatever the way in which it may have formed, the Ninetyeast Ridge is generally considered to be a dormant, fossil feature in the middle of a quiescent Indian plate. It is frequently cited as the prototype 'aseismic' ridge, where the aseismic ridges are a group of topographically high features which are not spreading ridges. Such features are especially common in the Indian Ocean (Chagos-Laccadive Ridge and Broken Ridge), but they occur in the other oceans as well (e.g., Walvis Ridge in the South Atlantic). All are aseismic in the sense that they do not show the many small earthquakes that make spreading ridges stand out on the recent (1964-1970) seismicity maps.

In a broader sense, when large earthquakes, over a longer period of time, are considered, the Ninetyeast Ridge is not aseismic but a rather seismic zone: historically, this area is far more seismic than any spreading ridge and, in fact, comparable in seismicity to large transform fault systems, such as the San Andreas fault. Only subduction zones are areas of greater total seismic activity, in terms of the number of large earthquakes.

Given this high level of seismicity, the area is either a zone of major intraplate deformation or an active plate boundary. We investigate the tectonics of this area by studying the mechanisms of 3 magnitude 7 and 3 magnitude 6 earthquakes in this area. Although three of these occurred many years ago (1928, 1939, and 1955) and are thus

Paper number 8B0129.
0148-0227/78/058B-0129$03.00

TABLE 1. Seismicity of the Ninetyeast Ridge Area

Date	Origin Time, GMT	Location	M_s	m_b	Source*
		$M_s \geq 7.0$			
Jan. 19, 1913	17:05:06	2°N, 86°E	7.0		GR
March 9, 1928	18:05:20	2.7°S, 88.7°E	7.7		location SO, magnitude GR
March 21, 1939	01:11:12	0.9°S, 89.5°E	7.2		location SO, magnitude GR
March 22, 1955	14:05:07	8.8°S, 91.7°E	7.0		location SO, magnitude G
		M_s = 6.0-7.0			
May 9, 1916	14:33:07	1.5°N, 89°E	6.3		GR
April 13, 1918	00:51:15	8°S, 85°E	6.5		GR
May 28, 1923	01:25:53	1.5°S, 88.5°E	6.5		GR
Jan. 18, 1926	21:07:23	2°S, 89°E	6.75		GR
Feb. 7, 1928	00:01:43	2.6°S, 88.5°E	6.75		location SO, magnitude GR
Jan. 23, 1949	06:31:04	11.6°S, 92.8°E	6.75		location SO, magnitude G
Sep. 1, 1950	02:46:55	4.5°S, 89.25°E	6.0		GR
May 25, 1964	19:44:07	9.1°S, 88.9°E	6.0	5.5	location CGS, magnitude UPP
Oct. 10, 1970	08:53:05	3.6°S, 86.2°E	6.2	5.9	location CGS, magnitude PAS
June 25, 1974	17:22:19	26.1°S, 84.3°E	6.2	6.2	GS
		$M_s < 6.0$			
Jan. 13, 1936	18:10:16	4°S, 85°E			GR
Jan. 25, 1951	16:35:36	1.5°S, 81.5°E			ISS
June 21, 1953	23:58:30	0.5°S, 91.4°E			ISS
Nov. 28, 1953	23:11:08	16.6°S, 93.1°E			ISS
March 23, 1955	04:54:33	8.7°S, 91.6°E			ISS
July 29, 1956	07:13:44	9.0°S, 85.5°E			CGS
June 26, 1957	02:47:37	7.3°S, 85.0°E			ISS
Jan. 11, 1964	10:23:11	11.4°S, 90.9°E			CGS
June 11, 1964	17:51:51	9.2°S, 89.5°E			CGS
Nov. 29, 1966	09:21:23	9.8°S, 90.6°E		5.0	CGS
April 23, 1967	15:01:06	1.6°N, 80.2°E		5.2	CGS
April 26, 1967	13:11:42	1.3°S, 89.4°E		5.0	CGS
Feb. 9, 1968	20:46:44	13.9°S, 82.4°E		5.1	CGS
Sep. 14, 1968	01:25:19	24.5°S, 80.4°E		5.5	CGS
Nov. 26, 1968	06:08:57	32.°S, 86.5°E			CGS
Dec. 14, 1968	11:43:14	3.1°S, 85.5°E		5.1	CGS
Jan. 3, 1969	03:56:59	18.2°S, 88.1°E		5.3	CGS
Feb. 14, 1969	06:14:53	17.8°S, 87.3°E		5.3	CGS
Dec. 3, 1972	17:58:56	11.3°S, 87.5°E		5.3	ERL
Dec. 14, 1972	20:49:35	1.3°S, 89.3°E		5.4	ERL
Oct. 29, 1973	07:07:36	28°S, 83.4°E			GS
June 25, 1974	18:31:36	25.8°S, 84.2°E		5.3	GS
June 26, 1974	05:59:25	26.0°S, 84.3°E		4.8	GS
June 26, 1974	09:07:26	26.0°S, 84.1°E			GS
June 28, 1974	08:45:44	25.8°S, 83.8°E		5.4	GS
Aug. 28, 1975	18:25:44	25.9°S, 84.2°E		5.4	GS

*SO, this study; GR, Gutenberg and Richter [1965]; G, B. Gutenberg (unpublished notepads); CGS, Coast and Geodetic Survey; NOS, National Ocean Survey; GS, U.S. Geological Survey; ERL, Environmental Research Laboratories; and ISS, International Seismological Summary.

difficult to study, we are able to extract enough information to learn a great deal about the tectonics of the area. Our seismological results are discussed in detail in the following three sections. These sections can be omitted by readers interested primarily in the present-day tectonics of the area.

Seismicity of the Ninetyeast Ridge Area

The Ninetyeast Ridge is not aseismic, as is easily demonstrated by the U.S. Geological Survey's world seismicity map [Tarr, 1974] which includes an event labeled 9 March 1928 (8.1) at about 3°S, 89°E. Gutenberg and Richter's [1965]

work, covering earthquakes from 1899 to 1952, shows several large events in this area. They state the following [Gutenberg and Richter, 1965, p. 78]:

> A peculiarly isolated group of shocks occurs near 2°S, 89°E...with other epicenters near 90°E north of the equator, there is suggested a minor seismic belt following imperfectly known rises and ridges roughly north and south.

The seismicity of this area is also discussed by Stover [1966], Rothé [1969], and Sykes [1970].

Using these sources, the worldwide magnetic tape catalog of epicenters, the 'Earthquake Notes' section of the Bulletin of the Seismological Society of America (1920-1963) and the International Seismological Summary (ISS)(1918-1963), we have compiled the seismicity list in Table 1. Since 1913, in the region from 80°E to 95°E and 5°N to 30°S (excluding the Sumatra trench) there have been 4 magnitude (M_S) 7, 10 magnitude 6, and at least 26 smaller earthquakes. The epicenter tape often does not include small ($M_S < 6$) events prior to 1950, for example, the aftershocks of the 1928 earthquake. In comparison, earthquakes along the midocean ridges almost never exceed surface wave magnitude 7, except infrequently on long transform faults [Gutenberg and Richter, 1965; Burr and Solomon, 1978].

A more useful comparison with Table 1 is to consider the entire Southern California fault system north of the Mexican border [Allen et al., 1965], including many faults in addition to the San Andreas, since 1912. If we add the Borrego Mountain and San Fernando earthquakes to bring their list up to date, there have been 18 events with $M_S > 6$ and 2 with $M_S > 7$. Thus in terms of moderate and large earthquakes the Ninetyeast Ridge (though a much larger area) is approximately as seismic as Southern California. (Smaller earthquakes in the central Indian Ocean are far less likely to be detected than those on land.)

A number of difficulties are involved in preparing a seismicity list such as Table 1. Clearly, the older earthquakes are subject to errors in location. Gutenberg and Richter [1965] state that 'location of even large shocks in this area is often difficult' because of the lack of nearby stations. As we discuss later, we have relocated several of the larger events. We feel (as did Gutenberg and Richter) that these events are definitely not in the Sumatra trench, the only other nearby region of high seismicity. Stover [1966] also relocated many of these events and determined that they were not associated with the trench. The locations in the table are from a variety of sources. Some (including three of the largest events) were relocated for this study. Otherwise, the Gutenberg-Richter location (for events prior to 1952) was used in preference to the ISS location. After 1952 the locations used are from the appropriate government agency or the International Seismological Summary (1952-1963), and later International Seismological Center (1964-1975).

The magnitude of these events is also a complicated issue, since magnitude is an often quoted but frequently ill-defined number. In the table we divide the earthquakes by surface wave magnitude into three groups: $M_S \geq 7$, $6 \leq M_S < 7$, and $M_S < 6$. This last group ('garbage earthquakes') also includes those for which no surface wave magnitude was determined, since they are almost certainly smaller than 6.

The determination of magnitude for historic earthquakes has been examined in detail by Geller and Kanamori [1977]. They show that the Gutenberg-Richter (GR) magnitudes given by Gutenberg and Richter [1965] are essentially equivalent to the modern 20-s surface wave magnitude but that the 'revised magnitude' frequently used is on the average 0.22 magnitude units higher. For example, the March 9, 1928, earthquake has a GR magnitude of 7.7 and a revised magnitude (shown on the U.S. Geological Survey [1974] map) of 8.1. For earthquakes after 1952 (when the records of Gutenberg and Richter [1965] end) and before 1958, it is sometimes possible to find the GR magnitude by examining Gutenberg and Richter's original worksheets, which are still available at the California Institute of Technology. The March 22, 1955, event, for example, has a GR magnitude of 7.0, although Rothé [1969] quotes the revised magnitude of 7.1.

The earthquakes in Table 1 are plotted in Figure 1 on the bathymetric map of Sclater and Fisher [1974]. Despite the uncertainty in locations (discussed later) a number of patterns are evident. The seismicity, especially the large events, trends roughly north-south, along the ridge. A large number of the earthquakes, including two of the largest, fall on the ridge itself. Many of the others are within a few degrees of the ridge. The large (M_S = 7 and 6) events are especially prone to be near the ridge. (Two of those farthest from the ridge are the poorly located 1913 and 1918 earthquakes.) There is also a noticeable concentration of events north of 10°S - all the magnitude 7 and 8 of 10 magnitude 6 events fall there. With the exception of the group of 1974 earthquakes at about 26°S (discussed in detail later), seismicity tends to occur north of 10°-12°S. As earthquakes of this size further south on the Southeast Indian Ridge are detected (as were the small aftershocks of the 1974 event), we feel that this is not an artifact of the seismic detection capability. There is also a suggestion that of the events not on the ridge, more occur on the west side than on the east size. In a later section we will attempt to relate these patterns to the bathymetry and tectonics of the area.

Earthquake Relocations

We have relocated five of the largest earthquakes in the area (3 magnitude 7 and 2 magnitude 6) for several reasons. Our primary concern was to show that these events are unlikely to be in the Sumatra trench. We also wished to test the published GR or ISS locations, which, before the era of computers, were obtained by a graphical technique [Richter, 1958]. In addition, we attempted to constrain the depth of these events, since focal depth is critical for our surface wave investigations [Tsai and Aki, 1970] as well as for tectonic purposes.

As we were able to collect only a small fraction of the original records, we used the arrival times published in the International Seismological Summary (1928-1955) for stations at distances less

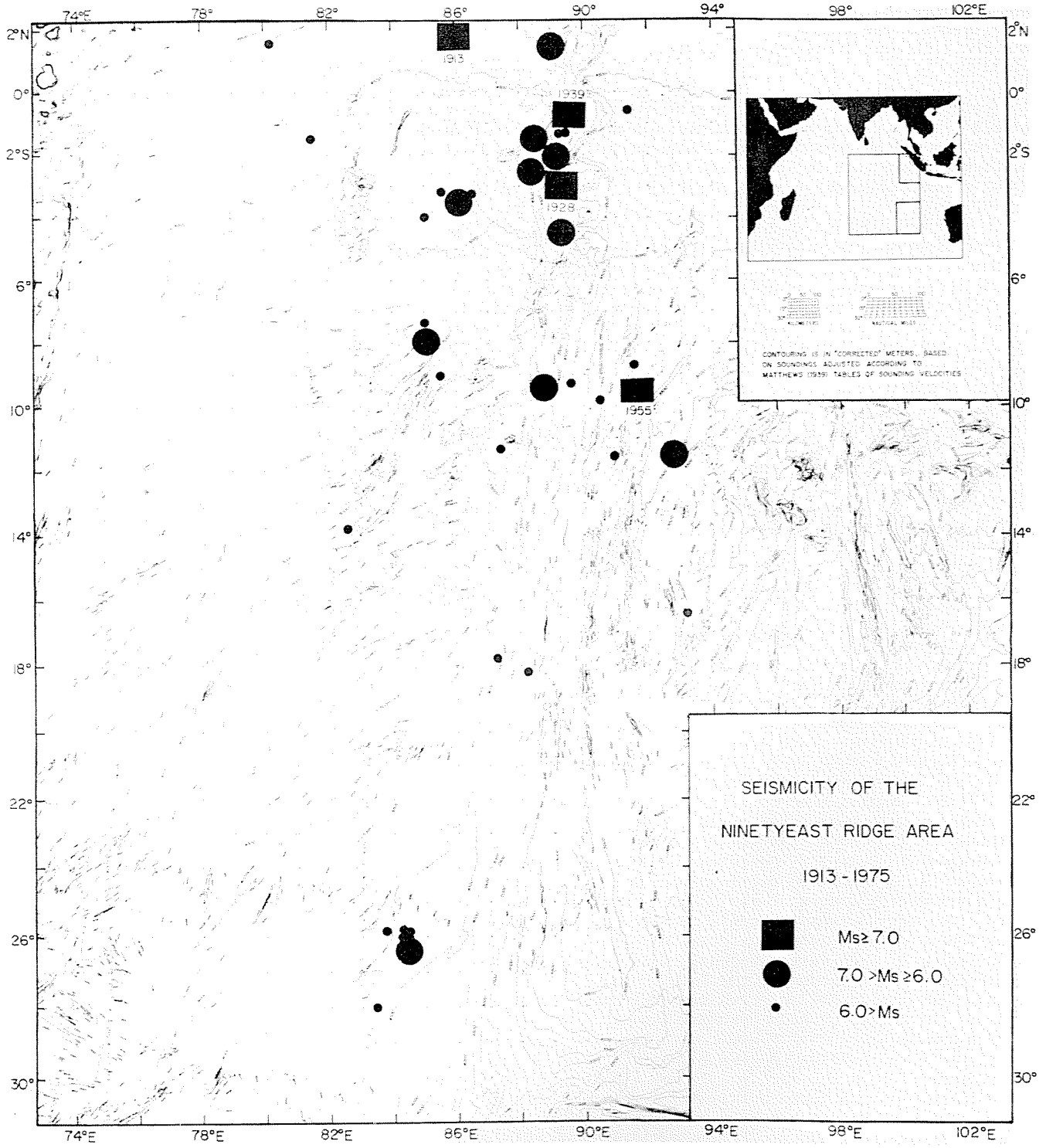

Fig. 1. Seismicity of the Ninetyeast Ridge area (Table 1) plotted on the bathymetric map of Sclater and Fisher. Earthquakes are divided into three groups on the basis of surface wave magnitude M_S.

than 90°. The ISS location and origin time were used as starting models. Locations were calculated by using a standard location program and a Jeffreys-Bullen travel time table.

The general procedure followed that of Kanamori and Miyamura's [1970] study of the 1923 Kanto earthquake. After the first iteration, all stations with travel time residuals greater than 30 s were suppressed. At this point the focal depth was then fixed at a series of depths, and the root-mean-square residual was calculated for each location. The same procedure was then repeated after deleting all stations with residuals greater than 10 s.

The results are shown in Figure 2. For each of the five events the rms residual is plotted as

a function of focal depth, for locations done after removing residuals greater than 30 s and then greater than 10 s. The figure also shows the number of stations used and their azimuthal distribution by quadrants. Unfortunately, the southern quadrants have very few stations, even today (see the focal mechanism for the 1974 event, Figure 3).

For all events the rms residual decreases as the source is placed at shallower depths. The results are much better for the 10-s case. Except for the 1955 event (where the change is too small to be significant) we interpret this as evidence of a shallow (less than 10 km) focal depth. This is in general accord with Burr and Solomon's [1978] result than transform fault earthquakes tend to occur at shallow depths.

The final locations and origin times for a 5-km focal depth are given in Table 1. The epicenters were quite stable with respect to changes in focal depth and in general differed only slightly (usually less than 0.5°) from the ISS (or GR) locations. For example, the March 9, 1928, location is given by the ISS as 2.3°S, 88.5°E; by GR as 2.5°S, 88.5°E, and by relocation as 2.6°S, 88.6°E. Similarly, the ISS located the 1955 event at 8.6°S, 91.6°E; B. Gutenberg (unpublished notepads), gives 9°S, 91.7°E; and the relocation yielded 8.8°S, 91.7°E. For smaller (or older) earthquakes the locations have greater uncertainties due to the small number of stations available. For example, the 1918 earthquake was recorded by 40 stations, of which only 26 reported P times. Gutenberg's location was 8°S, 85°E, in contrast to the ISS location of 5°S, 85°E, so the uncertainty is rather large. In contrast, the 1928 main shock was recorded by 121 stations, and the 1939 one by 147. For very old events, such as 1918, when only a small number of stations were available, we felt that no useful information would result from a relocation.

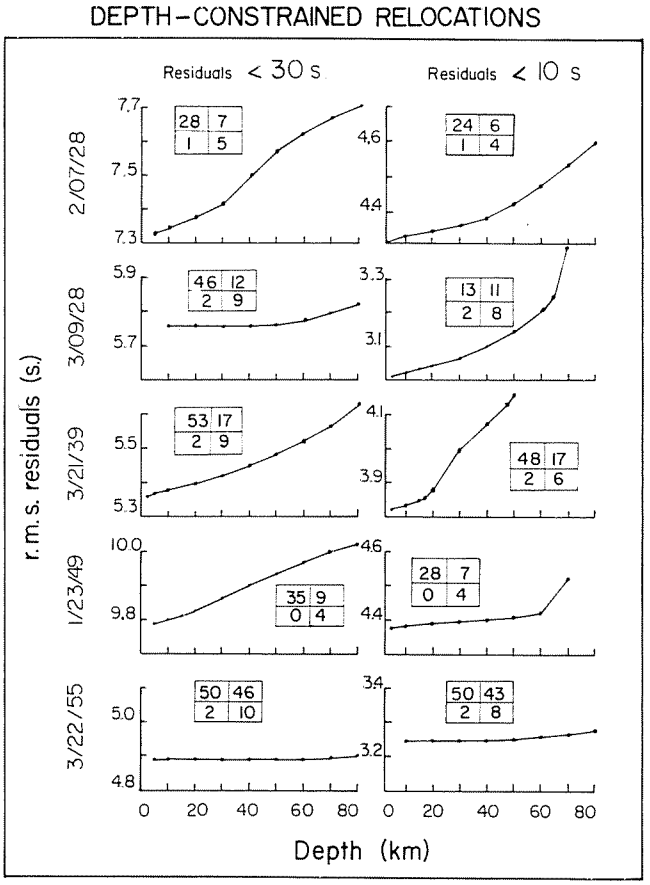

Fig. 2. Root-mean-square travel time residuals as a function of constrained depth during relocation of five large earthquakes in the Ninetyeast ridge area. (Left) relocation after deleting all stations with residuals greater than 30 s. (Right) Relocation after deleting stations with residuals greater than 10 s. In each plot the figures inside the box give the number of stations used in each azimuthal quadrant. The residuals decrease as the focus approaches the surface, suggesting that these earthquakes are shallow.

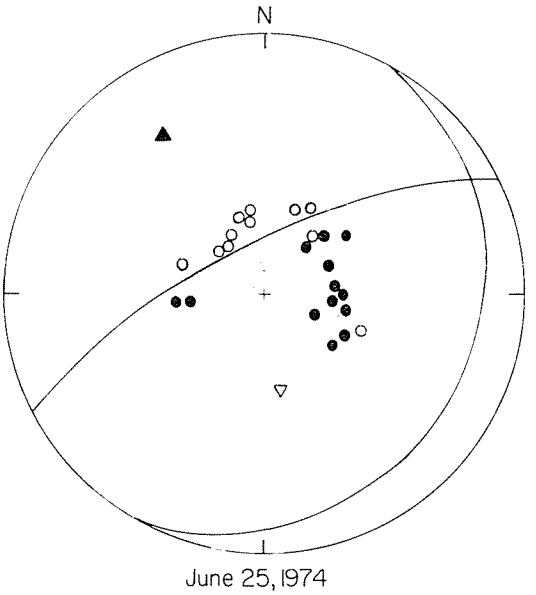

Fig. 3. Lower focal hemisphere plot of first-motion data for June 25, 1974. Solid circles are compressional, and open circles are dilatational. The second plane was constrained from surface wave data (see Figures 4 and 5). The solid triangle is the compressional axis, and the open one is the tensional axis.

Source Mechanism Studies

We studied the source mechanisms of two large earthquakes (March 21, 1939; M_S = 7.2 and March 22, 1955; M_S = 7.0) and one recent smaller event (June 25, 1974; M_S = 6.6). Study of the 1974 event, given the availability of records from many World-Wide Standard Seismograph Network (WWSSN) stations, followed the general methods of Kanamori [1970a, b]. The older events, for which only small numbers of records could be compiled, were studied using techniques similar to those of Kanamori [1970c] and Okal [1976, 1977].

For two of the older events (1939 and 1955) a small fraction of the stations reported first motions, as well as times, to the ISS. Care must be taken in using these pre-WWSSN results, since Wickens and Hodgson [1967] showed that stations were in error a significant portion of the time. We deleted from our first-motion solutions any

TABLE 2. Source Parameters for Major Recent Earthquakes in the Ninetyeast Ridge Area

Date	Origin Time, GMT	ϕ, deg	δ, deg	λ, deg	M_s	M_o, $\times 10^{25}$ dyn cm
March 9, 1928	18:05:20				7.7	400-800
March 21, 1939	01:11:12	166	82	57	7.2	200
March 22, 1955	14:05:07	244	80	-78	7.0	40
May 25, 1964*	19:44:07	266	80	0	6.0	1.1
Oct. 10, 1970†	08:53:00	126	83	164	6.2	2.9
June 25, 1974	17:22:19	242	74	97	6.6	2.5

*Focal mechanism from Sykes [1970].
†Focal mechanism from Fitch [1972].

stations whose travel time residuals exceeded 10 s. In drawing planes we gave heavy weight only to groups of stations which were internally consistent. Given these difficulties and the small number of stations reporting, only one plane could be reliably constrained from the first motions. We used surface wave data to determine the second plane and ensure the consistency of the plane derived from the first motions. Given the uncertainties in instrument response, only Love to Rayleigh wave amplitude ratios at single stations were used. Only for the 1974 event were amplitudes compared between different stations.

Unfortunately, we were unable to determine reliably the mechanism of the 1928 M_S = 7.7 earthquake, the largest reported in this area. In the absence of recorded first motions, the small set of records available that were usable for surface wave study was not adequate to constrain the solution reliably.

In the following sections we discuss the mechanism of each event, using the fault parameters strike ϕ, dip δ and slip angle λ defined by Kanamori and Cipar [1974]. We also determine the seismic moments of two earthquakes whose mechanisms were discussed previously in the literature. Table 2 presents a summary of our results.

June 25, 1974; M_S = 6.6

First-motion readings from 25 WWSSN stations (Figure 3) clearly constrain one of the planes near ϕ = 242°, δ = 74°. The compressional readings both in Japan and eastern Africa limit the slip angle to the range 25°-130°, thus restricting the strike slip component along the constrained plane.

For this fault plane, Figure 4 shows the azimuthal distribution of the nodes in the Love wave radiation pattern as a function of slip angle. Equalized seismograms from 22 records (Figure 5) exhibit a strong node at the European stations ESK, STU, COP and VAL constraining the slip angle to 97° ± 3°. The mechanism of the earthquake can then be considered a nearly pure thrust along a steeply dipping NE-SW fault. The seismic moment obtained from the equalized records is 2.5 × 10^{25} dyn cm.

March 22, 1955; M_S = 7.0

As noted earlier by Sykes [1970], the available first-motion data do not totally constrain the focal mechanism. An additional compressional reading was obtained from Lwiro, Zaire (LWI). Figure 6 shows that one plane has to lie somewhere between 233° (δ = 84°) and 244° (δ = 80°). The number of records suitable for a surface wave analysis is actually rather small. Love to Rayleigh wave amplitude ratios were obtained at two stations: De Bilt, Netherlands (DBN) and Resolute, Northwest Territories, Canada (RES), after low-pass filtering the records at both 30 and 60 s. This considerably reduces the dependence of the Rayleigh wave excitation with depth [Tsai and Aki, 1970]. The resulting values for L/R are 4 at RES (station azimuth, 1.9°) and 0.4 at DBN (station azimuth, 321.8°). Comparison with the theoretical values shown on Figure 7 as a function of slip angle yields λ = 102° (modulo 180°). The solution compatible with first-motion data is then (ϕ = 244°, δ = 80°, λ = -78°), a predominantly normal event along a steep NE-SW fault. This solution is also compatible with a strong, although uncalibrated, Rayleigh wave on the vertical Benioff short-period instrument at LWI. Using the instrument responses at DBN and RES, a seismic moment of 4 × 10^{26} dyn cm was obtained.

March 21, 1939; M_S = 7.2

Only 16 stations at distances less than 90° reported first motions to the ISS (Figure 8). The only strong constraint on the focal mechanism results from the clear separation between dilatational arrivals in southern Europe (Granada, Rome, Belgrade, Ksara, and Helwan) and compressional ones in northern Europe (Cernauti, Bucharest, Zurich, Strasbourg, De Bilt, and Paris). On a first-motion diagram, all these stations cluster together, and thus one fault plane must bisect them.

Excellent surface wave records at Christchurch, New Zealand (CHR), are shown on Figure 9. The Love to Rayleigh ratio is 0.8. Records at DBN, unfortunately, did not exhibit clean wave shapes after filtering, and as the amplitude ratios were unstable as a function of frequency, we decided against using them.

The Pasadena (PAS) record on the Benioff strainmeter (Figure 10) shows distinctive Love and Rayleigh waves, with a L/R ratio of 1.5.

Investigation of a large number of solutions generally consistent with the body wave constraint yielded the mechanism $\phi = 166°$, $\delta = 82°$, $\lambda = 57°$. Superficially, the data might appear insufficient to resolve the focal mechanism. However, given the location and origin time for a point source, it consists of a set of three parameters. Given the body wave constraint, two independent Love to Rayleigh amplitude ratios can (at least theoretically) yield the mechanism. The Pasadena record shows the dramatic sensitivity of L/R to slip angle, and the excellent fit of the synthetic to the original trace confirms the solution. An acceptable fit could not be obtained if, as the first motions might suggest, the plane were striking slightly further to the west. The final solution has a roughly north-south plane steeply dipping to the west, on which the motion is about one-half thrust and one-half left lateral strike slip.

The seismic moments obtained from CHR (2.6×10^{27} dyn cm) and PAS (1.5×10^{27} dyn cm) are in good agreement, especially in view of the problems associated with the strainmeter's calibration [Kanamori, 1976].

March 9, 1928; $M_S = 7.7$

No first-motion data were reported by the ISS in 1928. From the available records it appeared that WEL (Wellington) was compressional and COP (Copenhagen) and DBN were emergent. The other available records were difficult to interpret, especially since vertical instruments were quite rare in 1928. Love to Rayleigh ratios were obtained at WEL (2.5), DBN (0.8) and, despite a very low response at long periods, on the Wood-Anderson instrument at RVR (Riverside) (0.4). Love waves are present at La Paz, Bolivia (LPB), but no definite value could be obtained for the L/R ratio. Although several satisfactory focal solutions (generally similar to the solution for the 1939 event) can be found, the available data are insufficient to yield a unique mechanism. This is especially unfortunate, since comparison of the records from 1928 and 1939 at WEL (Figure 11) or DBN clearly shows that the 1928 event

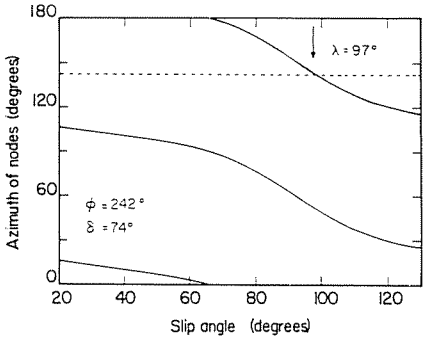

Fig. 4. Azimuth of nodes in the long-period Love wave radiation pattern as a function of slip angle along the fault plane constrained by first-motion data for June 25, 1974 ($\phi = 242°$, $\delta = 74°$). The dashed line is the observed node (see Figure 5).

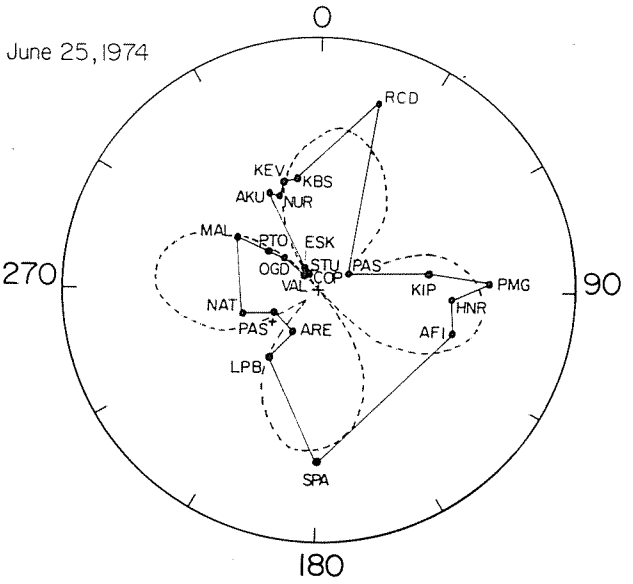

Fig. 5. Radiation pattern of equalized Love waves (G_1) for June 25, 1974, at 21 stations, using the technique of Kanamori [1970a, b]. PAS$^+$ denotes G_2 equalized to G_1. This figure yields the azimuth of the main Love wave node as $\phi = 141°$, which constrains the slip angle to $\lambda = 97°$, as shown on Figure 4. The resulting theoretical radiation pattern is shown as a dashed line.

was much larger than the 1939 one and contained more long-period energy. The large foreshock on February 7, 1928, and the numerous aftershocks (five were detected within a week, but the locations are uncertain) also suggest a very large earthquake. Estimates of the seismic moments computed by comparing a number of plausible mechanisms with the records at WEL or DBN fall in the range 4 to 8×10^{27} dyn cm.

May 25, 1964; $M_S = 6.0$

The pure strike slip mechanism of this event, obtained by Sykes [1970] from first motions, agrees well with both Rayleigh and Love wave radiation patterns. A sample of high-quality WWSSN records yields a seismic moment of 1.1×10^{25} dyn cm.

October 10, 1970; $M_S = 6.2$

The focal solution of this event (almost pure strike slip) was given by Fitch [1972] using first motions and S wave polarization angles. Records at PAS are consistent with this solution and yield a seismic moment of 2.9×10^{25} dyn cm. The moment of this event was determined from long-period SH wave spectra to be 6.7×10^{25} dyn cm [Richardson and Solomon, 1977].

Out of these six earthquakes, four (and presumably five) exhibit moment values systematically greater than would be expected from their 20-s surface wave magnitude. This suggests [Kanamori and Anderson, 1975] that the apparent stresses involved are 2-3 times lower than their world average, although a definite quantitative estimate is difficult to obtain. Unfortunately, it was not possible to infer any reliable value

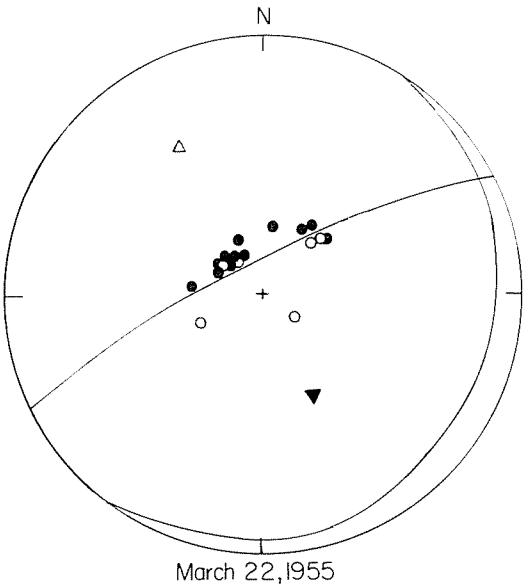

Fig. 6. Lower focal hemisphere plot of first-motion data for March 22, 1955. Symbols as defined in Figure 3. The second plane was constrained by surface wave data (see Figure 7).

of the stress drop $\Delta\sigma$, which has more direct physical meaning than the apparent stress: this quantity is usually obtained from estimates of the rupture area of the earthquake, which is difficult to measure in the absence of well-located aftershocks.

Tectonic Implications

In this section we attempt to describe the present-day tectonics of the area using the earthquake mechanisms and bathymetry. We propose a rather complex tectonic environment which seems generally consistent with the data.

Figure 12 shows our three fault mechanisms and the two others available in the literature for this area: Sykes's [1970] for the May 25, 1964, earthquake and Fitch's [1972] for the October 10, 1970, event. The figure also shows schematically several major morphological features of the area: the ridge, the zone of ridges and furrows to the west, the grabenlike deeps to the east, and the deep sea fans.

Along the northern (2°N-10°S) segment of the ridge, the most seismic area roughly corresponds to the area where the ridge is broken up into irregular blocks. The 1939 earthquake mechanism has about equal components of thrust and strike slip motion. We suggest that the thrusting is related to the irregular blocky nature of the ridge, and thus the southern aseismic portion of the ridge is much smoother and undeformed.

This relation between blocky morphology and recent deformation appears to continue to the north to 2°N. The ridge top sediments show evidence of recent faulting [Veevers, 1974]. Historic earthquakes were located in this area [Gutenberg and Richter, 1965], although we have excluded this northernmost segment from this study, owing to the difficulties in location in an area so close to the trench.

We interpret the strike slip motion as left lateral along a roughly north-south plane. This is consistent with the strike of the ridge and the general north-south alignment of seismicity and accords with the left lateral motion found for the 1964 earthquake further south. The alternate interpretation, strike slip and thrusting on the NE-SW plane, seems less plausible, although it would align roughly with the en échelon blocks on the ridge. Strike slip along the ridge's strike suggests that the deformation has some transform faultlike character as well as vertical motion resulting from compression across the ridge. This deformation seems to occur over a broad zone about the Ninetyeast Ridge rather than on a single sharply defined fault.

South of about 10°S, where the ridge changes in morphology and seismicity, we suggest that most of the intraplate deformation takes place off the ridge, leaving the ridge itself undeformed. Although the boundaries between the blocky and smooth ridge segments and the seismic and aseismic portions are not identical, they are close enough to suggest that they may be related. Tectonic structures not on the ridge cannot be seen north of 7°S owing to the thick fan sediments, so it is not clear whether a comparable boundary exists off the ridge.

If the NE-SW trending furrows and ridges to the west of the ridge are tectonic in origin, they suggest NW-SE compression. Few earthquakes occur in this region, so this compression appears to be primarily aseismic at present. The only major earthquake off the ridge and south of 10°S is the isolated 1974 shock. The thrust mechanism of this event is also consistent with NW-SE compression, but in the absence of detailed bathymetric data in the epicentral area, it is not possible to relate it to a particular structure. The April 13, 1918, earthquake was also located by Gutenberg and Richter in the furrow and ridge area, but little is known about this event, and owing to its date and size, its location may be inaccurate. The seismicity map (Figure 1) also suggests that off-ridge earthquakes occur more

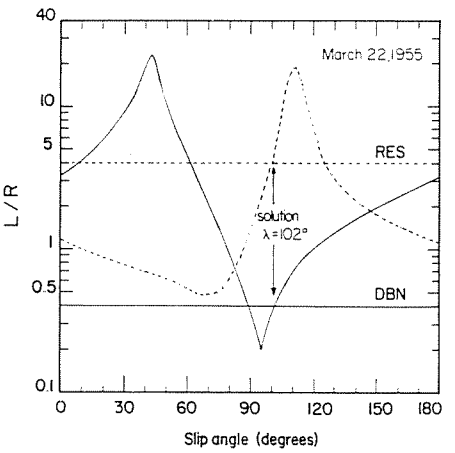

Fig. 7. Theoretical ratio of long-period Love to Rayleigh wave amplitudes as a function of slip angle along the fault plane obtained from first-motion data for March 22, 1955 (ϕ = 244°, δ = 80°). The solid curve is for DBN, and the dashed one is for RES. Horizontal lines indicate the observed values. The slip angle must satisfy both stations simultaneously.

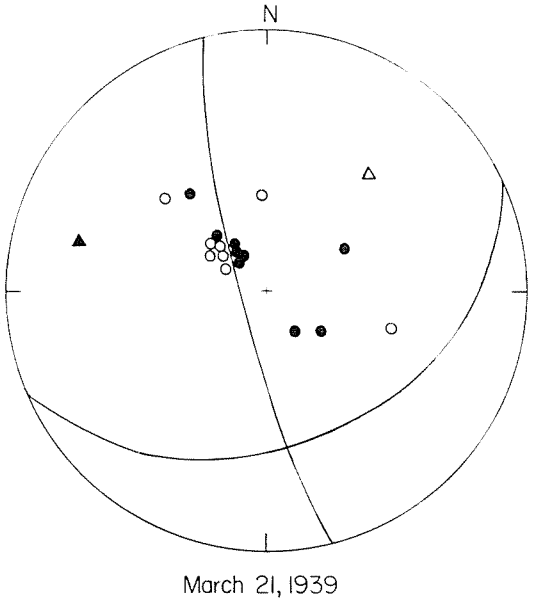

Fig. 8. Lower focal hemisphere plot of first-motion data for March 21, 1939. Symbols as defined in Figure 3. Both planes were obtained from surface wave data (see Figure 10), subject to the constraint imposed by the first motions.

frequently in this area than on the ridge's other side, but the total number of events is too small to show this conclusively.

The grabenlike troughs that roughly parallel the ridge on its east side, south of about 7°S, suggest tensional deformation. The normal fault mechanism of the 1955 earthquake in this area is also tensional, with tension in the NW-SE direction. This is in general accord with the trend of the troughs in the epicentral area, but neither the location accuracy or the bathymetry are adequate to assign this event to a specific feature. We propose that the graben formation is continuing today and that some fraction of this deformation occurs seismically.

The remaining portion of the Ninetyeast Ridge area that is covered by the sediment fans is difficult to discuss. The only moderate-sized earthquake which can confidently be located in this region is the 1970 event studied by Fitch [1972], who proposed strike slip motion consistent with north-south compression. (The 1913 earthquake was also located in the fan area, but as discussed earlier, the location is quite uncertain.) Deformation of the fan sediments themselves, suggesting north-south compression, was observed to the southeast (7°S, 80°E) by Eittreim and Ewing [1972].

The overall tectonics of the ridge and the ocean basin to the west can be crudely described if the west side is encountering resistance resulting from the Indian collision and the east side is subducting at the Sumatra trench. Such a situation would give rise to compression and left lateral motion in the region of the Ninetyeast Ridge if the ridge is the approximate boundary between the two sides. The situation is more complicated, since the compression seems to be

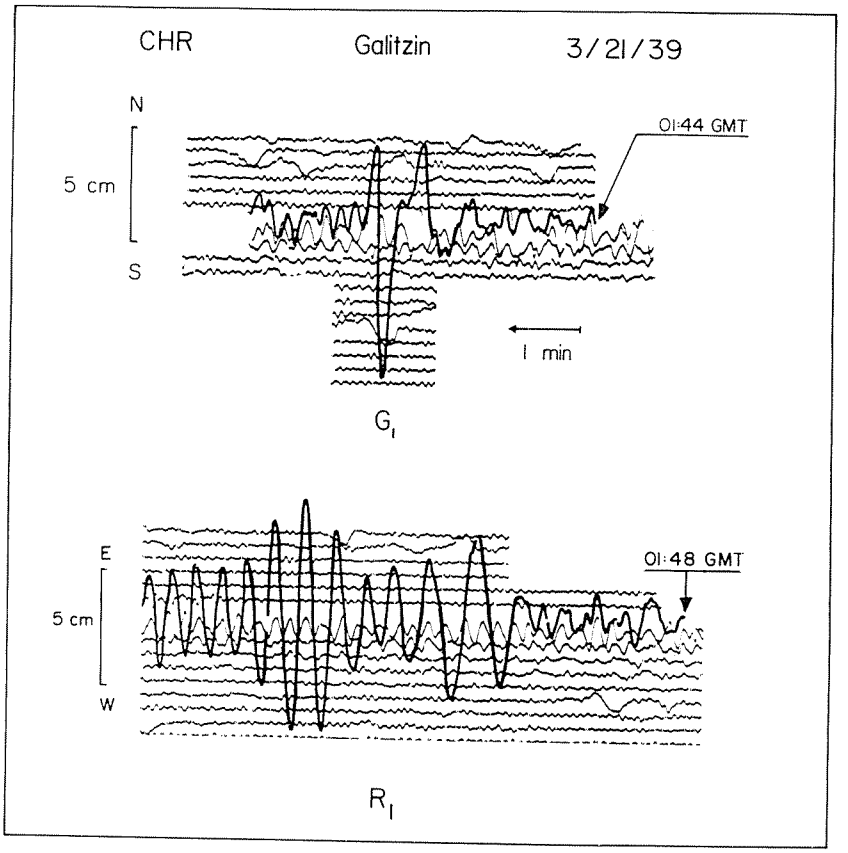

Fig. 9. Galitzin long-period records for March 21, 1939, at Christchurch, New Zealand.

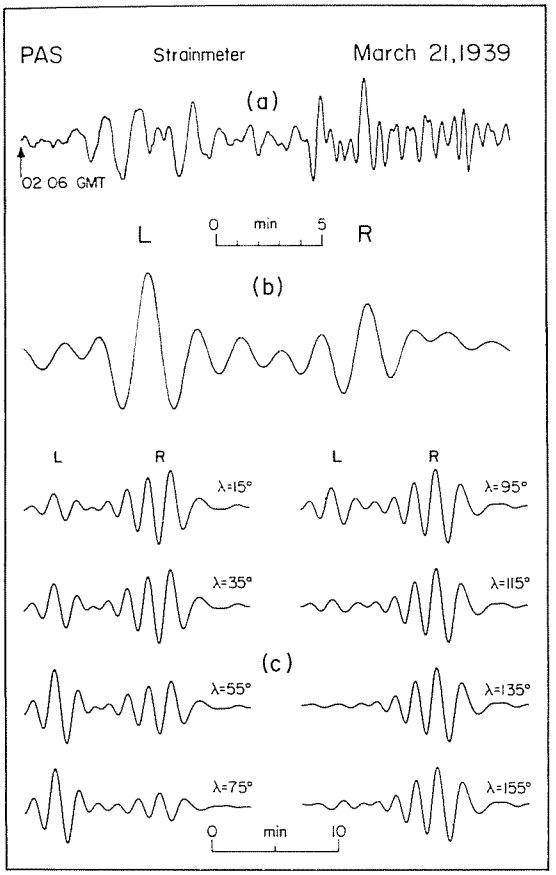

Fig. 10. (a) Original trace of the Benioff strainmeter at PAS for March 21, 1939. (b) Observed trace filtered at $T \geq 100$ s, showing Love wave (L) and Rayleigh wave (R) contributions to the north-south strain. (c) Synthetic seismograms obtained for various values of the slip angle λ along a fault plane defined by $\phi = 166°$, $\delta = 82°$. Note the extreme sensitivity to λ of the Love to Rayleigh ratio. The best fit is obtained for $\lambda \simeq 55°$.

occurring over a broad zone rather than precisely along the ridge. Thus although the ridge is presently behaving in some sense like a transform fault, it is not exactly one. It appears plausible that the present-day deformation would be concentrated about the old zone of weakness left by the transform fault.

Again, it may be worth recalling the San Andreas fault system. Although the general plate motion is along the transform fault, an entire complex of associated faults occurs nearby, frequently with senses of motion which differ from that of the San Andreas itself. The San Andreas system occurs in continental lithosphere, while the Ninetyeast Ridge deformation is occurring in old, thick oceanic lithosphere, in contrast to transforms near spreading ridges which are developed in young, thin oceanic lithosphere. This may be the reason why the present deformation near the Ninetyeast Ridge resembles that observed on land more than that observed at spreading ridges.

It is less clear what causes the tensional tectonics which we suggest occur to the east of the ridge. This may be related to the subduction at the Sumatra trench, since the north-south trending topography extends all the way to the trench [Sclater and Fisher, 1974], but it is difficult to explain the direction of the tension. In addition, closer to the trench, Fitch [1972] noted a strike slip event (2°N, 94.6°E) which also suggests east-west extension. The Sumatra trench is an extremely complex subduction zone along which the subduction is oblique and may be coupled to strike slip motion behind the trench [Fitch, 1972] and the opening of the Andaman Sea [Curray et al., 1978; Eguchi et al., 1978]. The trench is also interacting with the Indian plate and Ninetyeast Ridge in a very complex way.

Sykes [1970] studied the area of the Ninetyeast Ridge and suggested that its earthquakes might represent an incipient subduction zone forming between Australia and Ceylon. Our study uses additional data (the mechanisms of the 1939, 1955, and 1974 events) and recent bathymetric maps and proposes a different model. The earthquake locations, especially the large ones, appear to us to be near the Ninetyeast Ridge and oriented roughly north-south rather than northwest-southeast. The mechanisms of two (1939 and 1964) of the largest events show significant strike slip components. This is more suggestive of relative motion along the Ninetyeast Ridge than of nascent subduction. The 1974 thrust earthquake is also difficult to reconcile with incipient subduction. Only the 1955 event shows normal faulting, but this seems to be associated with the graben structures. Finally, no bathymetric evidence for an incipient subduction zone has been observed in the area [Sclater and Fisher, 1974].

Our model suggests that a significant fraction of the morphology of the Ninetyeast Ridge is due to the present-day tectonics of the area. Alternatively, Sclater and Fisher [1974] suggest that several of these features, including the en échelon nature of the northern segment of the ridge, are much older and may be related to the early history of the ridge. In our view the present seismic deformation is concentrated near the old ridge and transform fault and is modifying these preexisting features. We have no way of determining when this deformation began, and thus our results do not directly bear on the question of the origin of the ridge as a topographic high. It is possible, on the other hand, that the graben are completely the result of the present tectonic environment.

A possible difficulty with our interpretation is the time spanned by our seismic data. The spatial distribution of seismicity that we observe may not be representative. Even on a longer time scale, however, we would still expect the segment south of 9°S to be aseismic, on the basis of its smooth morphology.

This internal deformation of the Indian plate bears directly on the question of determining relative plate motions. The relative motions of all plates can be simultaneously found using plate boundary data by the method of least squares [Chase, 1972; Minster et al., 1974; Chase, 1978; Minster and Jordan, 1978], assuming all the plates are rigid. Minster and Jordan's [1978] solution yields inadequate closure of the triple junction. The failure of the junction closure suggests either inaccurate data or non-

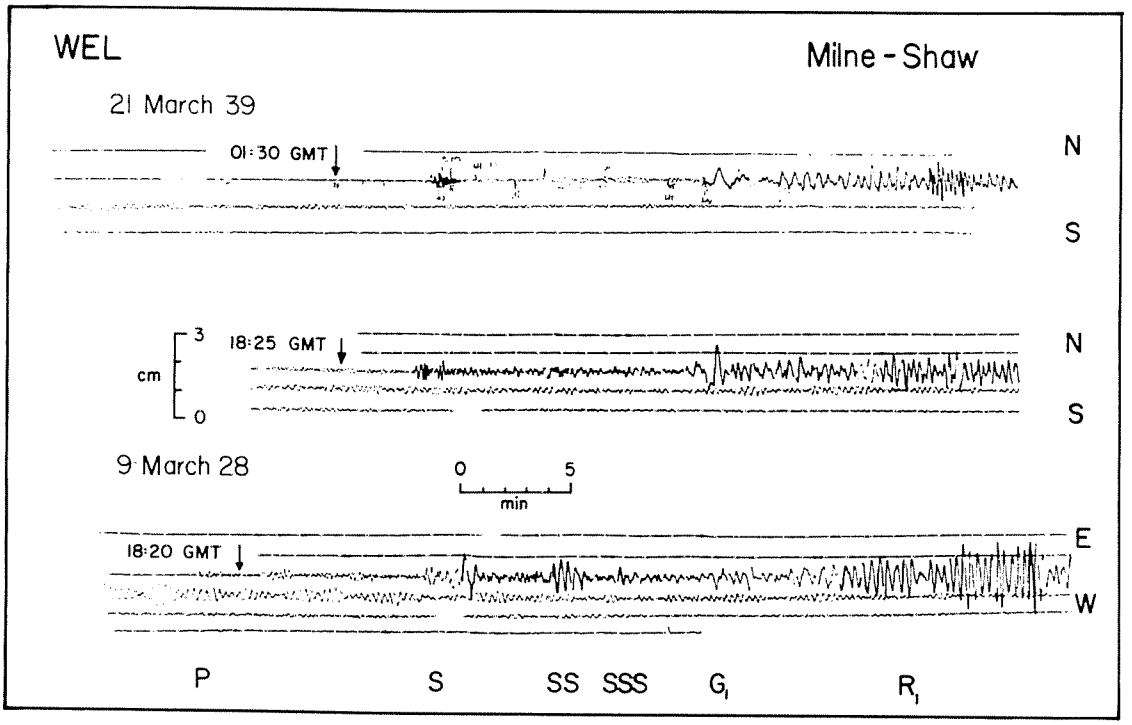

Fig. 11. A comparison of Milne-Shaw records at WEL for the March 21, 1939, and March 9, 1928, events. Principal seismic phases are identified. This figure illustrates the greater size of the 1928 event and the substantial long-period excitation from both events. The instrument magnification is 150.

rigid plates. Chase [1978] treats this problem using the opening of the African rift, while Minster and Jordan [1978] prefer internal deformation of the Indian plate. They split the Indian plate into West Indian and Australian plates and determine a pole between them which satisfies the relative motion data. No specific boundary is required by this analysis, but if the plate boundary were the Ninetyeast Ridge, NW-SE compression would occur across it. This prediction agrees with the earthquake mechanisms and our interpretation of the bathymetry.

A very crude estimate of the relative motion rate across the seismic portion of the ridge area can be obtained using a method suggested by Brune [1968]. We have determined the seismic moment for three earthquakes that appear to have been on the ridge (1928, 1939, and 1964) and thus have a rough relation between magnitude (M_S) and moment [Kanamori and Anderson, 1975]. We can then estimate the moment of other events from M_S. The total seismic moment along the ridge can be found by adding the 1923, 1926, 1928, and 1950 magnitude 6 events, which seem to have also been on the ridge (the pre-1923 locations seem too unreliable to justify using these earthquakes). It is worth noting that the total moment is almost completely due to the two largest events (1928 and 1939).

This total moment (8.6×10^{27} dyn cm) can be divided by the rigidity, the length of ridge (10°) over which the earthquakes occurred, and an assumed fault width. We estimated the depths at less than 10 km (which is reasonable for transform faults), so a conservative fault width would be 20 km. This yields 144 cm, over 41 years, or about 3.1 cm/yr. If we assume that half the motion is dip slip, division by $(2)^{1/2}$ yields 2.2 cm/yr of strike slip motion. Given the assumptions involved and the range of uncertainty in M_O, this should be regarded as only an order of magnitude estimate. It is approximately consistent with the rate (1 cm/yr) inferred from the triple junction misclosure [Minster and Jordan, 1978].

As this area appears to be the most active tectonic area within any of the oceanic plates, further study would be desirable. Ocean bottom seismometer experiments along the ridge and its flanks might explain a great deal about the present tectonics of this puzzling region.

Conclusion

The Ninetyeast Ridge area is a broad seismic zone considerably more active than the interior of any other oceanic plate. Focal mechanisms of the large earthquakes in the area suggest left lateral strike slip motion along the ridge and compression across it. The seismicity is concentrated in a zone paralleling the ridge, on its northern segment. To the south the ridge is aseismic, and deformation appears to occur on both sides. The bathymetry on the west side suggests compression, while that on the east side suggests tension. Mechanisms of earthquakes in these areas are in general agreement with this interpretation. The Indian plate is undergoing substantial internal deformation, with resolvable relative motion (at least in the seismic zone) between the Indian and the Australian side.

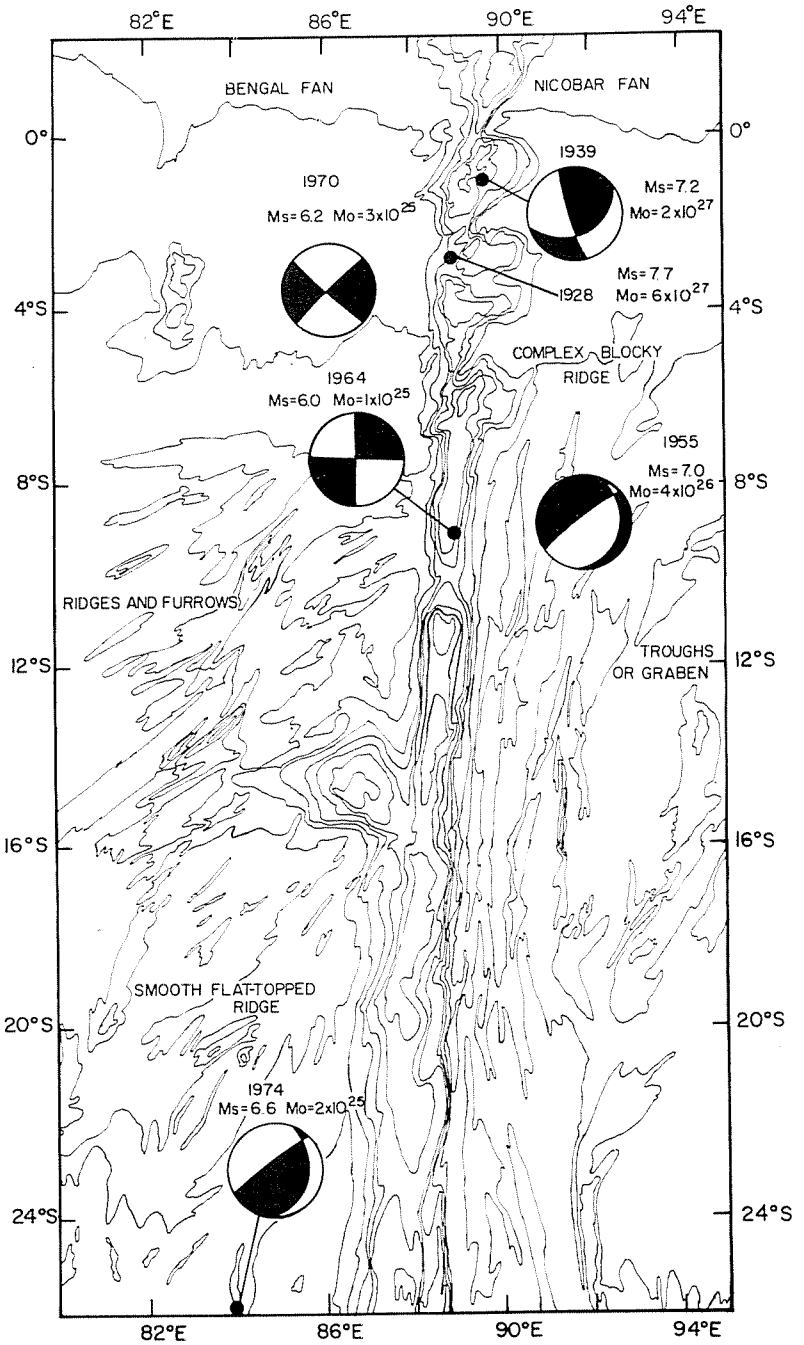

Fig. 12. Focal mechanism, magnitudes, and moments for major earthquakes near the Ninetyeast Ridge. The mechanism of the 1928 event could not be realiably determined. Note that the 1939 and 1964 events on the ridge show strike slip motion, the 1955 event is a normal fault, and the 1974 event is a thrust fault. The moments of the 1928 and 1939 earthquakes are much greater than any of the more recent events.

Acknowledgments. We thank Bob Geller, Yoshio Fukao, Hiroo Kanamori, Bernard Minster, and Tom Jordan for advice and assistance. R. L. Fisher supplied us with the bathymetric maps. Kazuya Fujita, Rob Cockerham, and Norman Sleep read the manuscript and made many valuable suggestions. We also thank the staff of many observatories around the world who provided us with seismograms and bulletins. Seth Stein was supported by a fellowship from the Fannie and John Hertz Foundation. This research was also supported by NSF grants EAR 76-14262 and EAR 77-13641. Contribution 2966, Division of Geological and Planetary Sciences, California Institute of Technology, Pasadena, California 91125.

References

Allen, C. R., P. St. Amand, C. F. Richter, and J. N. Nordquist, Relationship between seismicity and geologic structure in the southern California region, Bull. Seismol. Soc. Amer., 55, 753-797, 1965.

Bowin, C. O., Origin of the Ninetyeast ridge from studies near the equator, J. Geophys. Res., 78, 6029-6043, 1973.

Brune, J. N., Seismic moment, seismicity, and rate of slip along major fault zones, J. Geophys. Res., 73, 777-784, 1968.

Burr, N. C., and S. C. Solomon, The relationship of source parameters of oceanic transform earthquakes to plate velocity and transform length, J. Geophys. Res., 83, 1193-1205, 1978.

Chase, C. G., The N plate problem of plate tectonics, Geophys. J. Roy. Astron. Soc., 29, 117-122, 1972.

Chase, C. G., Plate kinematics: The America, East Africa, and the rest of the world, Earth Planet. Sci. Lett., in press, 1978.

Cockerham, R. S., B. P. Luyendyk, and R. D. Jarrad, Paleomagnetic study of sediments from site 253 DSDP, Ninetyeast Ridge (abstract), Eos Trans. AGU, 56(12), 978, 1975.

Curray, J. R., and D. G. Moore, Sedimentary and tectonic processes in the Bengal deep-sea fan geosyncline, in Geology of Continental Margins, edited by C. A. Burk and C. L. Drake, Springer, New York, 1974.

Curray, J. R., D. G. Moore, L. Lawver, F. Emmel, R. W. Raitt, and M. Henry, Tectonics of the Andaman Sea and Burma, Geology, in press, 1978.

Detrick, R. S., J. G. Sclater, and J. Thiede, The subsidence of aseismic ridges, Earth Planet. Sci. Lett., 34, 185-196, 1977.

Eguchi, T., S. Uyeda, and T. Maki, Seismotectonics and tectonic history of the Andaman Sea, Tectonophysics, in press, 1978.

Eittreim, S. L., and J. Ewing, Midplate tectonics in the Indian Ocean, J. Geophys. Res., 77, 6413-6421, 1972.

Fitch, T. J., Plate convergence, transcurrent faults and the internal deformation adjacent to Southeast Asia and the western Pacific, J. Geophys. Res., 77, 4432-4460, 1972.

Francis, T. J. G., and R. W. Raitt, Seismic refraction measurements in the southern Indian Ocean, J. Geophys. Res., 72, 3015-3041, 1967.

Geller, R. J., and H. Kanamori, Magnitudes of great shallow earthquakes from 1904 to 1952, Bull. Seismol. Soc. Amer., 67, 587-598, 1977.

Gutenberg, B., and C. F. Richter, Seismicity of the Earth and Associated Phenomena, Hafner, New York, 1965.

Kanamori, H., Synthesis of long-period surface waves and its application to earthquake source studies - Kurile Islands earthquake of October 13, 1963, J. Geophys. Res., 75, 5011-5025, 1970a.

Kanamori, H., The Alaskan earthquake of 1964: Radiation of long-period surface waves and source mechanism, J. Geophys. Res., 75, 5029-5040, 1970b.

Kanamori, H., Seismological evidence for a lithospheric normal faulting - The Sanriku earthquake of 1933, Phys. Earth Planet. Interiors, 4, 289-300, 1970c.

Kanamori, H., Reexamination of the earth's free oscillations excited by the Kamchatka earthquake of November 4, 1952, Phys. Earth Planet. Interiors, 11, 216-226, 1976.

Kanamori, H., and D. L. Anderson, Theoretical basis of some empirical relations in seismology, Bull. Seismol. Soc. Amer., 65, 1073-1095, 1975.

Kanamori, H., and J. J. Cipar, Focal process of the great Chilean earthquake, May 22, 1960, Phys. Earth Planet. Interiors, 9, 128-136, 1974.

Kanamori, H., and S. Miyamura, Seismometrical reevaluation of the great Kanto earthquake of September 1, 1923, Bull. Earthquake Res. Inst. Tokyo Univ., 48, 115-125, 1970.

Le Pichon, S., and J. R. Heirtzler, Magnetic anomalies in the Indian Ocean and sea floor spreading, J. Geophys. Res., 73, 2101-2117, 1968.

Luyendyk, B. P., and T. A. Davies, Results of DSDP leg 26 and the geologic history of the southern Indian Ocean, in Initial Reports of the Deep Sea Drilling Project, vol. 26, edited by T. A. Davies et al., U.S. Government Printing Office, Washington, D. C., 1974.

Luyendyk, B. P., and W. Rennick, Tectonic history of aseismic ridges in the eastern Indian Ocean, Geol. Soc. Amer. Bull., 88, 1347-1356, 1977.

Minster, J. B., and T. H. Jordan, Present-day plate motions, in press, J. Geophys. Res., 1978.

Minster, J. B., T. H. Jordan, P. Molnar, and E. Haines: Numerical modelling of instantaneous plate tectonics, Geophys. J. Roy. Astron. Soc., 36, 541-576, 1974.

Morgan, W. J., Deep mantle convection plumes and plate motions, Amer. Ass. Petrol. Geol. Bull., 56, 203-213, 1972.

Okal, E. A., A surface wave investigation of the Gobi-Altai (December 4, 1957) earthquake, Phys. Earth Planet. Interiors, 12, 319-328, 1976.

Okal, E. A., The July 9 and 23, 1905, Mongolian earthquakes: A surface wave investigation, Earth Planet. Sci. Lett., 34, 326-331, 1977.

Peirce, J. W., The northward motion of India since the late Cretaceous, Geophys. J. Roy. Astron. Soc., 52, 277-312, 1978.

Richardson, R. M., and S. C. Solomon, Apparent stress and stress drop for intraplate earthquakes and tectonic stress in the plates, Pure Appl. Geophys., 115, 317-331, 1977.

Richter, C. F., Elementary Seismology, W. H. Freeman, San Francisco, 1958.

Rothé, J. P., Seismicity of the Earth, UNESCO, Paris, 1969.

Sclater, J. G., and R. L. Fisher, The evolution of the east central Indian Ocean, with emphasis of the tectonic setting of the Ninetyeast Ridge, Geol. Soc. Amer. Bull., 85, 683-702, 1974.

Stover, C. W., Seismicity of the Indian Ocean, J. Geophys. Res., 71, 2575-2581, 1966.

Sykes, L. R., Seismicity of the Indian Ocean and a possible nascent island arc between Ceylon and Australia, J. Geophys. Res., 75, 5041-5055, 1970.

Tarr, A. C., World Seismicity Map, United States Geological Survey, Washington, D. C., 1974.

Tsai, Y. B., and K. Aki, Precise focal depth determination from amplitude spectra of surface waves, J. Geophys. Res., 75, 5729-5743, 1970.

Veevers, J. J., Seismic profiles made underway on leg 22, in Initial Reports of the Deep Sea Drilling Project, vol. 22, edited by C. C. van der Borch et al., pp. 351-368, U.S. Government Printing Office, Washington, D. C., 1974.

Wickens, A. J., and J. H. Hodgson, Computer Re-evaluation of Earthquake Mechanism Solutions, 1922-1962, Dominion Observ., Ottawa, Ont., 1967.

(Received September 2, 1977;
revised January 9, 1978;
accepted January 23, 1978.)